INTERBAND ABSORPTION OF LIGHT IN BISMUTH NANOSTRUCTURES

N. B. Mustafayev[1,2]

[1]*Institute of Physics, Azerbaijan National Academy of Sciences, Baku, Azerbaijan*
[2]*Physics Department, Azerbaijan National Academy of Aviation, Baku, Azerbaijan*
e-mail: nadirmustafayev@gmail.com

(Received 11 September 2012)

Abstract

Interband absorption of light in bismuth nanostructures has been studied in the framework of a complex model for electron spectrum of Bi, such as the Cohen model, the Abrikosov-Falkovsky model, and the McClure model. The obtained results differ qualitatively from those obtained in the framework of simple band models, such as the parabolic band model and the Lax two-band model. It is shown that both the interband transition with quantum number conservation and the interband transition without quantum number conservation are allowed in the framework of complex models for electron energy spectrum of Bi. Due to the interband transitions without quantum number conservation (these transitions are forbidden in simple band models), the peak of optical absorption in measured spectra can occur at lower photon energies than in the spectra simulated in the framework of simple band models. A similar difference between the peaks was observed by Black et al. in Bi nanowires. The interband transitions without quantum number conservation substantially complicate the oscillation pattern and the identification of absorption peaks. The frequency dependence of the coefficient of interband absorption calculated in the framework of the McClure model has pronounced peaks, whereas in the simple band models this dependence has a step-like pattern. It is concluded that the McClure model enables the oscillation behavior of interband absorption in bismuth nanostructures to be properly described.

1. Introduction

Bismuth is a semimetal with a small band overlap and a very anisotropic electron effective mass tensor. For a bismuth structure of small enough thickness for significant quantum confinement to occur, the structure undergoes a transition from a semimetal with a small band overlap to a semiconductor with a small direct band gap. This transition, as well as other quantum effects, occurs in bismuth structures at relatively large thicknesses because of the small effective mass and small band overlap of bulk bismuth.

Bismuth nanostructures are promising for optical applications because of their unusual properties. For example, quantum wells, quantum dots, and quantum wires usually have to be doped in order to populate the lowest subband and to allow for optical excitation of the electrons to higher subbands. In bismuth nanostructures, the lower subbands are partially filled with electrons, and intersubband transitions can be observed even in undoped samples.

It should be noted that many commonly used approximations are not valid for bismuth. For example, a simple parabolic band model is not applicable for the description of electron energy spectrum at the *L*-point of the Brillouin zone, since the *L*-point electronic bands are extremely anisotropic and have strong nonparabolic effects. Several models were proposed to describe the

energy spectrum of Bi [1]: the Lax model (this model is also called the ellipsoidal nonparabolic model), the Cohen model (or the nonellipsoidal nonparabolic model), the Abrikosov-Falkovsky model, the McClure model, and the McClure-Choi model.

The Lax model is a comparatively simple two-band model. This model is often used for studying quantum size effects in Bi films [2] and wires [3-5]. The Lax model makes it possible to obtain qualitative but not quantitative agreement with experimental results. For example, the local minimum in the transmission, which corresponds to a peak in the optical absorption, occurs at higher photon energies in the calculated spectra compared to the experimentally measured spectra [5]. A possible explanation for the discrepancy is that the Lax two-band model is unable to take into account the far-band contributions.

The aim of the present paper is to study optical absorption in bismuth nanostructures in the framework of complex models taking into account the far-band contributions. It follows from calculations that the results obtained in the framework of the complex models (such as the Cohen model, the Abrikosov-Falkovsky model, and the McClure model) differ qualitatively from the results obtained in the framework of the simple models (such as the parabolic model and the Lax model).

For example, in the framework of simple models, the threshold of interband absorption is defined as $\hbar\omega_0 = E_g + 2E_F$, where E_g is an energy gap at the *L*-point of the Brillouin zone, and E_F is the Fermi energy. This is because only interband transitions with the selection rule $N_v = N_c$ (where N_v is an initial state in the valence band, and N_c is a final state in the conduction band) are allowed in the simple models. In the framework of the complex models, interband transitions with both the selection rule $N_v = N_c$ and the selection rule $N_v + N_c = 2l + 1$ (where l is an integer) are allowed; therefore, the interband absorption at frequencies less than ω_0 becomes possible.

The frequency dependence of the coefficient of interband absorption $\alpha(\omega)$ in Bi quantum wells calculated in the framework of complex models has pronounced peaks, whereas the dependence $\alpha(\omega)$ calculated in the framework of simple models does not have these peaks. In simple models, as it is known, this dependence has a step-like pattern [6].

2. Energy spectrum

The Fermi surface of electrons in Bi consists of three valleys tilted at a small angle with respect to the basal plane. The valleys transfer into each other under a rotation of $\pm 120^\circ$ around the trigonal z axis. If the quantization axis is parallel to z, the wave function for electrons can be tried in the form of a one-column matrix with elements $C_j U_j f_j(z) \exp(ik \cdot \rho)$, where $k = (k_x, k_y, 0)$ and $\rho = (x, y, 0)$, the x axis is parallel to the binary axis, the y axis is parallel to the bisectrix axis (the small tilt angle may be neglected), U_j are the Bloch functions, C_j are unknown coefficients and $f_j(z)$ are unknown functions which can be derived from a solution of the differential equation system obtained using an effective Hamiltonian of the energy spectrum model. If the Bloch functions have the same value at both boundaries of quantum-well structure, the condition of size quantization takes the quasi-classical form. In this case, the conduction and valence bands are described by wave functions of the form

$$\psi^{j}_{\mathbf{k},N} = \exp(ik\cdot\rho)\left(A^{j}_{\mathbf{k},N}\sin\frac{\pi Nz}{d} + B^{j}_{\mathbf{k},N}\cos\frac{\pi Nz}{d}\right). \quad (1)$$

Here N is a quantum number, d is the thickness of quantum-well structure. The explicit forms of $A^{j}_{\mathbf{k},N}$ and $B^{j}_{\mathbf{k},N}$ are determined by the model parameters and the Bloch functions. The cumbersome expressions for $A^{j}_{\mathbf{k},N}$ and $B^{j}_{\mathbf{k},N}$ are not given here.

It should be noted that, for the complex models of energy spectrum, it is necessary to impose a zero boundary condition for the total wave function rather than for the envelopes. In the case of simple models, the zero boundary condition for envelopes $f_j(0)=f_j(d)=0$ coincide with the zero boundary condition for the total wave function $\psi(\rho,0)=\psi(\rho,d)=0$. However, in the case of complex models, these conditions do not coincide with each other. It is impossible to construct all $f_j(z)$ simultaneously in the form of partial solutions. The functions $f_j(z)$ are related to each other via the initial set of equations. It may be shown that the zero boundary condition for the total wave function leads to the following boundary condition for the envelopes:

$$\left\{1+R_j(z_0)\nabla_z\right\}f_j(z_0)=0. \quad (2)$$

Here z_0 has two values: $z_0=0$ and $z_0=d$. There is a relation between $R_j(z_0)$ and the values of the Bloch functions fixed at the boundaries of quantum-well structure. Condition (2) coincides formally with those obtained in [7]. In [7], the quantity R is a real constant (with the dimension of length) which yields information about surface properties of crystals.

One can derive the electron spectrum in quantum-well structure from solution of the Schrödinger equation using the effective Hamiltonian of the energy spectrum model. From calculations made, for example, using the effective Hamiltonian of the McClure model [8], it follows that the electron energy spectrum is of the form

$$\left(E-\frac{\alpha_c}{2}k_y^2\right)\left(E+E_g+\frac{\alpha_v}{2}k_y^2\right)=Q_{11}^2k_x^2+Q_{22}^2k_y^2+Q_{33}^2\left(\frac{\pi N}{d}\right)^2. \quad (3)$$

Here Q_{ii} are matrix elements of the velocity operator which characterize the $\kappa\cdot p$ interaction between the valence and conduction bands in the three principle directions, α_c and α_v are the free electron and far-band contributions to the inverse band-edge effective mass of the conduction and valence bands, respectively, in the direction of the isoenergetic surface elongation. The parameters of the McClure model were determined in [9].

3. Optical absorption

The coefficient of interband absorption calculated in the framework of complex models is of the form $\alpha=\alpha_1+\alpha_2$, where α_1 corresponds to transitions with the selection rule $N_v=N_c$, and α_2 corresponds to the transitions with the selection rule $N_v+N_c=2l+1$ (Fig. 1b). This occurs because, for direct interband transitions, the dipole matrix elements calculated using (1) are of the form

$$\left\langle\sigma_c\,N_c\left|\,p_i\,\right|\sigma_v N_v\right\rangle = M_{1,i}\delta_{N_cN_v}+M_{2,i}\kappa_{N_cN_v}. \quad (4)$$

Here σ_v and N_v are the spin and quantum numbers of the initial state in valence band, σ_c and

N_c are the spin and quantum numbers of the final state in conduction band, $M_{1,i}$ and $M_{2,i}$ are cumbersome expressions,

$$\delta_{N_c N_v} = \begin{cases} 0; & N_c \neq N_v \\ 1; & N_c = N_v \end{cases}$$

$$\kappa_{N_c N_v} = \begin{cases} 0; & N_c - N_v = 2l \\ \dfrac{2d}{\pi} \dfrac{N_c N_v}{(N_c + N_v)(N_c - N_v)}; & N_c - N_v = 2l+1 \end{cases}$$

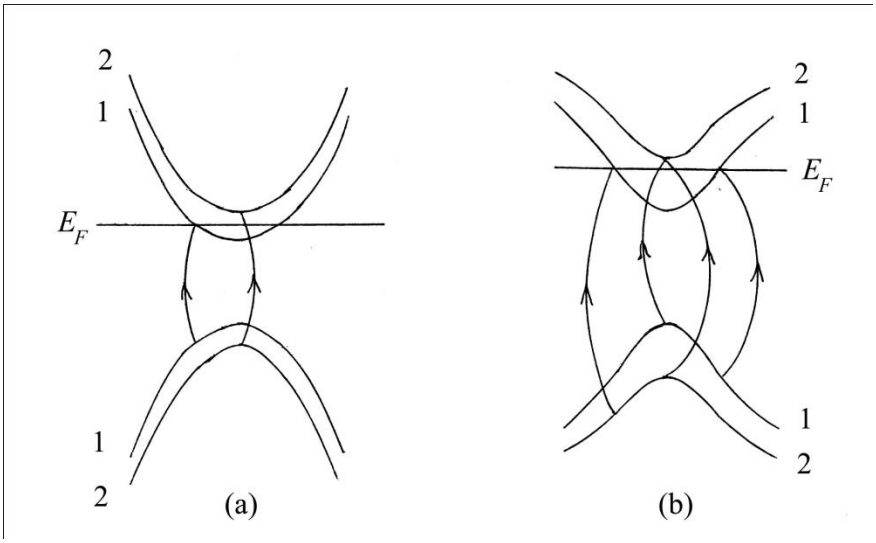

Fig. 1. Interband transitions in (a) simple and (b) complex models for the energy spectrum of Bi quantum-well structures.

If the polarization vector is parallel to the binary axis ($i = x$), the expression for α_1 is of the relatively simple form

$$\alpha_1 = \alpha_0 \sum_N \sqrt{1-2m}\, K(m) H(\chi). \tag{5}$$

Here

$$\alpha_0 = \frac{3}{2}\left(\frac{4e^2}{nc\hbar d}\right) \frac{Q_{11}}{\sqrt{E_g(\alpha_c + \alpha_v) + 4Q_{22}^2}},$$

n is the index of refraction, c is the velocity of light, $K(m)$ is the first complete elliptic integral, $H(\chi)$ is the Heaviside function,

$$m = \frac{b^2}{a^2 + b^2},$$

$$a^2 = b^2 + \frac{2}{\mu+1} + \frac{4\lambda}{(\mu+1)^2},$$

$$\mu = \frac{\alpha_v}{\alpha_c},$$

$$\lambda = \frac{2Q_{22}^2}{E_g \alpha_c},$$

$$\eta = \frac{\hbar\omega}{E_g},$$

$$\varepsilon_0 = \frac{\pi Q_{33}}{E_g d},$$

$$b^2 = \frac{1}{\mu+1}\left(-\frac{\mu+1+2\lambda}{\mu+1} + \sqrt{\left(\frac{\mu+1+2\lambda}{\mu+1}\right)^2 + \eta^2 - 1 - 4\varepsilon_0^2 N^2}\right),$$

$$\varepsilon_F = \frac{E_F}{E_g},$$

$$\varepsilon_N = \frac{1}{2}\left(-1+\sqrt{1+4\varepsilon_0^2 N^2}\right),$$

$$\chi = \begin{cases} \eta - 1 - 2\varepsilon_N ; & \varepsilon_F < \varepsilon_1 \\ \eta - 1 - 2\varepsilon_F ; & \varepsilon_F > \varepsilon_1 \end{cases}$$

The expression for α_2 is of rather cumbersome form, so it is not given here. Though $\alpha_2 < \alpha_1$, the interband transitions without quantum number conservation substantially complicate the oscillation pattern and the identification of absorption peaks.

To simplify the problem, consider here only the case where $\varepsilon_F < \varepsilon_1$. From the solution of the electroneutrality equation at helium temperature, it follows that the Fermi level is located below the bottom of the first subband if $d = 30$ nm, where the overlap between the L and T bands disappears and the Bi quantum-well structure undergoes a semimetal-semiconductor transition. The frequency dependence of the coefficient of interband absorption calculated in the framework of the McClure model for a 30-nm-thick quantum-well structure at helium temperature is plotted in Fig. 2 It is evident from this figure that the frequency dependence has pronounced peaks.

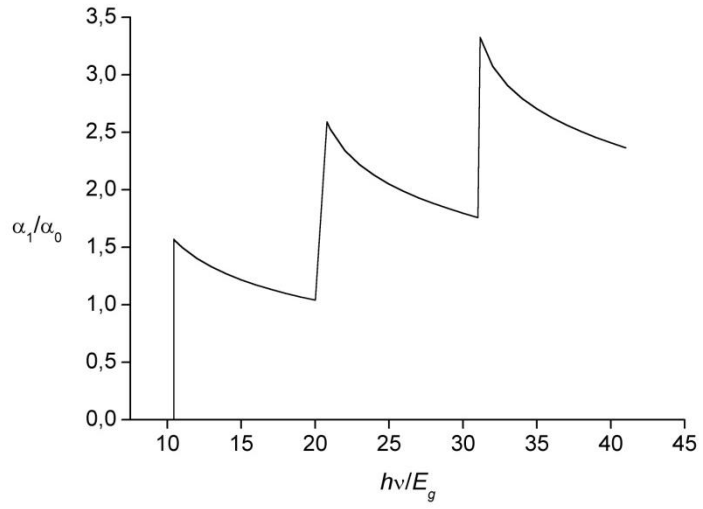

Fig. 2. Frequency dependence of the coefficient of interband absorption calculated in the framework of the McClure model for a 30-nm-thick Bi quantum-well structure at helium temperature.

4. Discussion

Optical absorption in thin Bi films under the conditions of a quantum size effect was first observed in [10]. In [10], the spectral dependence of transmission of the Bi films evaporated on a KBr substrate was measured at room temperature. The following results were obtained: a shift of the red edge of the optical absorption upon the variation in film thickness d, a semimetal-semiconductor transition at $d = 30\,\text{nm}$, a nonmonotonic spectral dependence of the optical transmission, and a shift of the absorption maximum near the absorption edge with changing film thickness. The results were qualitatively explained in the framework of the parabolic band model.

A further research of the optical absorption in Bi films was made in [11, 12]. In [11], a blueshift of the IR absorption measured on Bi films epitaxially grown on BaF_2 substrates was observed. From far-infrared reflectivity, the plasma frequencies ω_p of films as a function of film thickness d were determined. With decreasing film thickness, ω_p initially increased and then abruptly decreased near $d = 10\,\text{nm}$. This was considered as a sign of a semimetal-semiconductor transition caused by the quantum size effect.

In [12], the reflectivity and transmittivity of thin monocrystalline bismuth films on barium fluoride were measured in a spectral range of 80 to $4000\,\text{cm}^{-1}$. The measurements were performed at room temperature and at 5 K. At 5 K, thickness-dependent absorption maxima occurred at the film thickness less than 50 nm. These maxima were interpreted as transitions between subbands of the valence and conduction bands at the *L*-points of the Brillouin zone. The spectral position of the maxima was explained assuming an elevated gap energy due to the lattice mismatch between the films and the substrates.

Optical absorption in Bi nanowires prepared inside the pores of anodic alumina was studied in [3-5]. In [3, 4], the contributions to the optical absorption from both intersubband and direct interband transitions were modeled, and the results were compared to the measured absorption spectra. The theory for the absorption resulting from a direct interband transition did not show agreement with the experimentally measured data. The smaller intensity absorption peaks were thus attributed to optical absorption resulting from intersubband transitions, but the intersubband theory did not explain the large peak near $\sim 1000\,\text{cm}^{-1}$. The magnitude of the energy shift of this peak with a change in wire diameter, as well as the overall shape of the absorption spectra near this absorption peak, was not explained.

In [5], the optical absorption resulting from indirect transitions was studied in order to explain the observed spectra. Although the spectra simulated and measured in [5] are similar, the local minimum in the transmission, which corresponds to a peak in the optical absorption, occurs at a higher photon energy in the simulated spectra than in the experimentally measured spectra. For example, in 45-nm-diameter wires at room temperature, the wave numbers of the simulated and measured absorption peaks differ by $\sim 400\,\text{cm}^{-1}$. This difference can result from approximations used in [5]. For example, the approximation of the *L*-point bands by the Lax two-band model makes it impossible to take into account the contributions from bands outside of the two-band model.

Infrared transmission spectroscopy measurements on single bismuth nanowires of various diameters *d* were presented in [13]. The strong absorption signal was attributed to interband transitions. The blueshift was assigned to quantum size effects leading to the *d*-dependent splitting of the energy bands and to a respective shift of energy gaps.

In [3-5] and [10-13], the experimental results were analyzed in the framework of simple models (the parabolic band model and the Lax two-band model). The complex models (such as the Cohen model, the Abrikosov-Falkovsky model, and the McClure model) were not used. In [14-16], we used the Cohen model and the Abrikosov-Falkovsky model to study optical absorption and electronic Raman scattering in thin Bi films. In the present paper, the McClure model is used. It follows from calculations that the results obtained in the framework of the complex models qualitatively differ from the results obtained in the framework of the simple models.

For example, only interband transitions with quantum number conservation are allowed in simple models (Fig. 1a); therefore, the threshold of interband absorption is defined as $\hbar\omega_0 = E_g + 2E_F$. In the framework of complex models, both the interband transition with quantum number conservation and the interband transition without quantum number conservation are allowed; so, the interband absorption at frequencies less than ω_0 is possible.

As an illustration, consider the simple situation (Fig. 1b) where only the first subband is filled. The energy for electron transition from the state $N_v = 1$ to the state $N_c = 2$ ($\hbar\omega = E_g + E_{c,2}$) is less than the energy for electron transition from the state $N_v = 1$ to the state $N_c = 1$ ($\hbar\omega_0 = E_g + 2E_F$). If E_F is near the bottom of the second subband, the difference in energy $\hbar(\omega_0 - \omega) \approx E_F$.

According to [4], in 41.5-nm-diameter wires at room temperature, the Fermi energy E_F lies 48 meV above the lowest *L*-point conduction band minimum. Therefore, the difference in energy between the interband transition with quantum number conservation and the interband transition without quantum number conservation is $\hbar(\omega_0 - \omega) = 387\ \text{cm}^{-1}$. This value is in close agreement with the difference ($\sim 400\ \text{cm}^{-1}$) in wave numbers of the simulated and measured absorption peaks in 45-nm-diameter wires [5]. Thus, due to the interband transitions without quantum number conservation, the peak of optical absorption in measured spectra can occur at lower photon energies than in the spectra simulated in the framework of the Lax model. These transitions are forbidden in the Lax model, but they are allowed in the framework of complex models.

The frequency dependence of the coefficient of interband absorption calculated in the framework of the complex models has pronounced peaks (Fig. 2). The dependence $\alpha(\omega)$ calculated in the framework of simple models does not have these peaks. In simple models, as it is known, this dependence has a step-like pattern [6]. Thus, complex models of electron spectrum describe the oscillation behavior of interband absorption in low-dimensional Bi structures better than the parabolic band model and the Lax two-band model.

5. Conclusions

In the framework of complex models for electron energy spectrum of Bi, such as the Cohen model, the Abrikosov-Falkovsky model, and the McClure model, both the interband transition with quantum number conservation and the interband transition without quantum number conservation are allowed. Due to the interband transitions without quantum number conservation (these transitions are forbidden in simple band models), the peak of optical absorption in measured spectra can occur at lower photon energies than in the spectra simulated in the

framework of simple band models. The interband transitions without quantum number conservation substantially complicate the oscillation pattern and the identification of absorption peaks. The frequency dependence of the coefficient of interband absorption calculated in the framework of the complex models has pronounced peaks, whereas in simple band models this dependence has a step-like pattern. The use of the McClure model makes it possible to properly describe the oscillation behavior of interband absorption in low-dimensional Bi structures.

References

[1] Edel'man V.S., Sov. Phys. Usp. 20, 819 (1977).
[2] Zaluzny M. and Lukasik A., Phys. Status Solidi B 137, 607 (1986).
[3] Black M.R., Padi M., Cronin S.B., Lin Y.-M., Rabin O., McClure T., Dresselhaus G., Hagelstein P.L., and Dresselhaus M.S., Appl. Phys. Lett. 77, 4142 (2000).
[4] Black M.R., Lin Y.-M., Cronin S.B., Rabin O., and Dresselhaus M.S., Phys. Rev. B 65, 195417 (2002).
[5] Black M.R., Hagelstein P.L., Cronin S.B., Lin Y.-M., and Dresselhaus M.S., Phys. Rev. B 68, 235417 (2003)
[6] Davies J.H., The Physics of Low-Dimensional Semiconductors: An Introduction, Cambridge, University Press, Cambridge, 1998.
[7] Volkov V.A. and Pinsker T.N., Sov. Phys. JETP 43, 1183 (1976).
[8] McClure J.W., J. Low Temp. Phys. 25, 527 (1976).
[9] Akhmedov S.Sh., Herrmann R., Kashirin K.N., Krapf A., Kraak V., Ponomarev Ya.G., and Subakova M.V., Sov. Phys. JETP 70, 370 (1990).
[10] Lutskii V.N. and Kulik L.A., JETP Lett. 8, 80 (1968)
[11] Takaoka S. and Murase K., J. Phys. Soc. Japan 54, 2250 (1985).
[12] Peschke Ch., Phys. Status Solidi B 191, 325 (1995).
[13] Cornelius T.W., Toimil-Molares M.E., Neumann R., Fahsold G., Lovrincic R., Pucci A., and Karim S., Appl. Phys. Lett. 88, 103114 (2006).
[14] Mustafaev N.B. and Shakhtakhtinskii M.G., Phys. Status Solidi B 124, K151 (1984).
[15] Gadzhiev A.T., Gashimzade F.M., and Mustafaev N.B., Solid State Phys. 30, 3146 (1988).
[16] Gadzhiev A.T., Gashimzade F.M., and Mustafaev N.B., J. Phys.: Condens. Matter 3, 4677 (1991).